Published in final edited form as:
Glia. 2014 August ; 62(8): 1227–1240. doi:10.1002/glia.22675.

Astrocytic transforming growth factor-beta signaling reduces subacute neuroinflammation after stroke in mice

Egle Cekanaviciute[1,2], **Nancy Fathali**[1], **Kristian P. Doyle**[1], **Aaron M. Williams**[1], **Jullet Han**[1], and **Marion S. Buckwalter**[1,3]

[1] Department of Neurology and Neurological Sciences, Stanford University School of Medicine, Stanford, CA, 94305-5489

[2]Neurosciences Graduate Program, Stanford University, Stanford, CA, 94305-5489

[3]Department of Neurosurgery, Stanford University School of Medicine, Stanford, CA, 94305-5489

Abstract

Astrocytes limit inflammation after CNS injury, at least partially by physically containing it within an astrocytic scar at the injury border. We report here that astrocytic transforming growth factor-beta (TGFβ) signaling is a second, distinct mechanism that astrocytes utilize to limit neuroinflammation. TGFβs are anti-inflammatory and neuroprotective cytokines that are upregulated subacutely after stroke, during a clinically accessible time window. We have previously demonstrated that TGFβs signal to astrocytes, neurons, and microglia in the stroke border days after stroke. To investigate whether TGFβ affects astrocyte immunoregulatory functions, we engineered "Ast-Tbr2DN" mice where TGFβ signaling is inhibited specifically in astrocytes. Despite having a similar infarct size to wildtype controls, Ast-Tbr2DN mice exhibited significantly more neuroinflammation during the subacute period after distal middle cerebral occlusion (dMCAO) stroke. The peri-infarct cortex of Ast-Tbr2DN mice contained over 60% more activated $CD11b^+$ monocytic cells and twice as much immunostaining for the activated microglia and macrophage marker CD68 than controls. Astrocytic scarring was not altered in Ast-Tbr2DN mice. However, Ast-Tbr2DN mice were unable to upregulate TGF-β1 and its activator thrombospondin-1 two days after dMCAO. As a result, the normal upregulation of peri-infarct TGFβ signaling was blunted in Ast-Tbr2DN mice. In this setting of lower TGFβ signaling and excessive neuroinflammation, we observed worse motor outcomes and late infarct expansion after photothrombotic motor cortex stroke. Taken together, these data demonstrate that TGFβ signaling is a molecular mechanism by which astrocytes limit neuroinflammation, activate TGFβ in the peri-infarct cortex, and preserve brain function during the subacute period after stroke.

Corresponding author: Marion S. Buckwalter, MD PhD Departments of Neurology and Neurological Sciences, and Neurosurgery Stanford University School of Medicine 1201 Welch Road Stanford, CA 94305-5489 Tel: (1) 650 724 9098, Fax: (1) 650 498 6262 marion.buckwalter@stanford.edu.

Conflict of Interest: none.

Main Points: Astrocytic TGFβ signaling is a critical pathway for limiting subacute neuroinflammation in peri-infarct cortex after stroke. Mice with inhibited astrocytic TGFβ signaling exhibited excessive neuroinflammation, failed to upregulate TGFβ, and developed worse motor deficits after stroke.

Keywords

Astrocytes; cytokines; immunity; ischemia; inflammation

Introduction

Astrocytes are uniquely positioned to regulate inflammatory responses after CNS injury. They become activated during the subacute period after injury that is characterized by neuroinflammation (Barreto et al. 2011; Chen and Swanson 2003) and respond to injury in a highly localized manner. Previous research in our laboratory demonstrated that after stroke astrocytes in the peri-infarct cortex respond to the major regulatory cytokine transforming growth factor-beta (TGFβ), as measured by nuclear localization of its downstream mediator phosphorylated Smad2 (pSmad2) in glial fibrillary acidic protein (GFAP)-expressing astrocytes (Doyle et al. 2010; Massagué and Wotton 2000). However, the functions of astrocytic TGFβ signaling during the subacute period after stroke remain to be discovered.

Astrocytes react to injury by increasing GFAP expression. $GFAP^+$ astrocytes eventually form a physical barrier, also known as the astrocytic scar, which limits immune cell infiltration and protects adjacent uninjured tissue (Schachtrup et al. 2010; Sofroniew and Vinters 2010). This process of astrocytic scar formation requires astrocytic STAT3 and GFAP (Li et al. 2008; Wanner et al. 2013).

In addition to forming a scar, astrocytes respond to CNS injury by producing pro-inflammatory cytokines and chemokines. For example, astrocytes produce the chemokines CCL2, CXCL1 and CXCL2 after ischemia or spinal cord injury (Pineau et al. 2010; Zamanian et al. 2012), and CCL2 and CCL5 after traumatic brain injury (Babcock et al. 2003; Glabinski et al. 1996). These pro-inflammatory chemokines may be beneficial by attracting immune cells, which have been shown to reduce tissue damage by clearing dead cells (Dheen et al. 2007; Iadecola and Anrather 2011). On the other hand, excessive inflammation can be harmful by inducing free-radical damage to neurons (Brown 2010) and increasing cerebral edema, which can cause brain herniation and further tissue damage (Heiss 2012). Therefore, it is essential to limit neuroinflammation during the subacute period after injury in order to reduce neuronal damage.

We hypothesized that the activation of astrocytic TGFβ signaling that we observed in the subacute period after stroke might represent an active anti-inflammatory function of astrocytes. The TGFβ isoform TGF-β1 is upregulated by the majority of brain injuries (Finch et al. 1993) and signals to all cell types in the injured brain (Buckwalter and Wyss-Coray 2004; Pratt and McPherson 1997). It is specifically increased during the subacute period that coincides with neuroinflammation after stroke (Yamashita et al. 1999). TGFβs have anti-inflammatory functions in the immune system (Crowe et al. 2000; Fadok et al. 1998) and are acutely neuroprotective at the time of stroke (Pang et al. 2001; Ruocco et al. 1999). However, TGFβ functions in astrocytes during the subacute period after stroke are not known.

To investigate how endogenous TGFβ signaling regulates astrocyte function after stroke *in vivo*, we engineered a transgenic mouse model to inhibit TGFβ signaling in $GFAP^+$ astrocytes during the subacute period after stroke by expressing a mutant receptor that is unable to initiate downstream signaling when bound by either TGFβ isoform (Frugier et al. 2005; Shi and Massague 2003). Temporal specificity was achieved using a GFAP promoter that is upregulated in the peri-infarct cortex during this time. We demonstrate that inhibiting astrocytic TGFβ signaling resulted in excessive immune cell infiltration and activation 2-3 days after stroke. This increase in neuroinflammation was not associated with changes in infarct size, or in astrocytic GFAP upregulation and scar formation. However, inhibiting TGFβ signaling abolished the normal upregulation of TGF-β1 and its activator thrombospondin-1, and blunted TGFβ pathway activation in the peri-infarct cortex. Finally, inhibiting astrocytic TGFβ signaling was also associated with worse motor outcomes. We conclude that TGFβ signaling is critical for astrocytic control of neuroinflammation and preserving function in the peri-infarct cortex during the subacute period after stroke.

Materials and Methods

Mice

All use of animals was conducted according to protocols approved by the Stanford Institutional Animal Care and Use Committee and the NIH Guide for Care and Use of Animals. Ast-Tbr2DN transgenic mice were a cross between the lines B6.FVB-Tg(tetOEGFP,-Tgfbr2)8Mcle/J (JAX #005738) and B6.Cg-Tg(GFAP-tTA)110Pop/J (JAX #005964), both obtained from Jackson Labs. The first line (Frugier et al. 2005; Lin and Yang 2013; Rani et al. 2011) carries a bi-tetO promoter that drives the expression of two genes: a dominant negative mutant Type II TGFβ receptor, which has a truncated intracellular domain and prevents all TGFβ signaling (Shi and Massague 2003), and enhanced green fluorescent protein (eGFP). Thus, eGFP expressing cells are also expected to express high levels of the mutant receptor. The second transgenic line expresses GFAP-tTA, which directs bi-tetO promoter-mediated expression to $GFAP^+$ astrocytes (Florian et al. 2011; Halassa et al. 2009; Pascual et al. 2005). Similar to the native GFAP promoter, the GFAP promoter in GFAP-tTA mice strongly increases transgene expression after injury (Brenner et al. 1994). All experiments were done using two month-old females. Singly transgenic B6.FVB-Tg(tetO-EGFP,-Tgfbr2)8Mcle/J mice were used as wildtype littermate controls.

Surgery

Distal middle cerebral artery occlusion (dMCAO) strokes were induced as previously described (Doyle et al. 2010). For photothrombotic stroke, the skull was cleaned of connective tissue and lightly shaved using a sterile razor blade. The Dolan-Jenner MH- 100 Metal Halide Fiber Optic Illuminator (Edmundoptics, #56371) light source with a 5 mm diameter optic cable (Edmundoptics, #39365) was placed on top of the skull and 40 × microscope objective was used to focus the light. The light was turned on twice for 15 minutes, beginning 5 minutes after a 40 mg/kg Rose Bengal (Sigma, #330000-5G) injection (10 mg/ml in sterile saline, administered intraperitoneally), to form two overlapping circular lesions in the right motor cortex. Body temperature was maintained at 37°C, and

immediately following surgery mice received 10 mg/kg of Cefazolin (VWR, #89149-888) and 0.1 mg/kg of Buprenorphine (Henry Schein, #6030894) for infection prophylaxis and pain management.

Flow cytometry

We homogenized the stroked hemisphere and collected a monocyte-enriched population of cells using a Percoll gradient (Arac et al. 2011). The cells were stained with the following markers and antibodies: AquaAmine Live/Dead stain (Invitrogen, #L34957) CD11b-PE (eBioscience, #12-0112-82) and CD45-APC (eBioscience, #17-0451-82), counted on the FACSAria III cell sorter (BD Biosciences) and analyzed using FlowJo software (TreeStar).

Perfusion and brain processing for immunohistochemistry

Mice were sedated with 3.8% chloral hydrate and terminally perfused with 0.9% NaCl containing 10 U/mL heparin. Brains were fixed in 4% paraformaldehyde in phosphate buffer for 24 hours, rinsed with PBS, and then sunk in 30% sucrose in PBS. Coronal brain sections 40 μm thick were cut using a freezing sliding microtome (Microm HM430) into 24 sequential tubes, so that each tube contained every 24^{th} section spaced 960 μm apart, and were stored in cryoprotective medium at −20°C.

Immunohistochemistry

We analyzed images with MetaMorph and ImageJ software. We evaluated GFAP co-localization with eGFP and with pSmad2 in 4 coronal sections per mouse, evenly spaced 480 μm apart. To avoid bias, co-localization of pSmad2 with GFAP was scored first, and eGFP expression was examined afterwards. We quantified CD68 immunostaining in the peri-infarct cortex in 5 sections per mouse at 2.5× magnification, evenly spaced 960 μm apart. We quantified GFAP immunostaining in the peri-infarct cortex in 2 sections per mouse at 2.5× magnification, 960 μm apart. We counted $MHCII^+$ cells in 3 sections per mouse 960 μm apart.

Infarct size evaluation

Infarct size was quantified using an immunostain with an anti-NeuN antibody that marks neuronal nuclei, counterstained with cresyl violet, which marks all cell nuclei. The infarct was traced on 6 sections per mouse, 480 μm apart, and expressed as % of the ipsilateral hemisphere after dMCAO (Woo et al. 2012) or as volume after photothrombotic stroke (Clarkson et al. 2011).

Antibodies

We used the following primary antibodies for immunohistochemistry: anti-phosphorylated Smad2 (rabbit, 1:1000, Millipore, #AB3849), anti-GFAP (rabbit, 1:1000, DAKO, #Z0334), biotinylated anti-GFAP (mouse, 1:200, Abcam, #ab79203), anti-eGFP (chicken, 1:200, Millipore, #AB16901), biotinylated anti-NeuN (mouse, 1:200, Millipore, #MAB377B), anti-CD68 (rat, 1:1000, Serotec, #MCA1957S), anti-MHCII (rat, 1:500, BD Pharmingen, #553621), anti-NG2 (rabbit, 1:500, Millipore, #AB5320), and anti-phosphoAkt (rabbit, 1:1000, Abcam, #ab81283).

We used the following secondary antibodies for immunohistochemistry: AlexaFluor-488 donkey anti-chicken (Jackson Immunoresearch, #703-096-155), AlexaFluor-555 streptavidin (Invitrogen/Molecular Probes, #S-32355), AlexaFluor-555 donkey anti-rabbit (Invitrogen, #A31572), AlexaFluor-555 donkey anti-rat (Jackson Immunoresearch, #712-165-153), AlexaFluor-647 donkey anti-rabbit (Invitrogen, #A-31573), AlexaFluor-647 streptavidin (Invitrogen/Molecular Probes, #S-21374), and biotinylated rabbit anti-rat (Vector Laboratories, #BA-4001).

We used the following antibodies for Western blots: phosphorylated Smad2 (rabbit, 1:200, Millipore, #AB3849), Smad2 (rabbit, 1:200, Cell Signaling, #3122), phosphorylated Akt (mouse, 1:200, Cell Signaling, #4051), Akt (rabbit, 1:200, Cell Signaling, #9272), actin (rabbit, 1:20,000, Sigma, #A5060), goat anti-rabbit HRP (1:20,000, Santa Cruz, #sc-2004) and goat anti-mouse HRP (1:20,000, DAKO, #P0447). Actin was used as a loading control.

Sample preparation for protein and mRNA measurements

After perfusion, we dissected tissue samples from the peri-infarct cortex and the contralateral cortex directly opposite the stroke core, as well as from cortex and striatum in sham mice. The peri-infarct cortex was defined as the cortical area within 2.5 mm radius from the stroke core at the time of tissue extraction.

For protein assays, tissue was flash frozen and kept at −80°C until homogenization in cell lysis buffer with Complete Mini protease inhibitor (Roche, #11836153001) and 0.1% Na_3VO_4. Samples were sonicated for 10 seconds, centrifuged at 14000 rpm for 10 minutes, and the protein concentration in the supernatant was equalized using a BCA Pierce protein assay kit (ThermoScientific, #23227). Four to six animals per group were used for all protein assays. For Western blots, tissue lysates were mixed with 20% dithiothreitol in 4x NuPage LDS loading buffer (Invitrogen, #NP0007). Samples were loaded onto 4–12% NuPage Bis-Tris gels (Invitrogen, #NP0335) and subsequently transferred onto polyvinylidene fluoride membranes (Amersham, #RPN303F).

Multiplex luminex assay and ELISA

Multiplex luminex assay was performed by the Human Immune Monitoring Center at Stanford University (himc.stanford.edu). Each sample was measured in duplicate. Plates were read using a Luminex 200 instrument with a lower bound of 100 beads per sample per cytokine. Results were analyzed using Cluster 3.0 and visualized using JavaTreeView software. TGF-β1 protein concentration was measured using a Mouse/Rat/Porcine/ Canine TGF-β1 Quantikine ELISA kit (R&D Systems, #MB100B). To activate latent TGF-β1, protein samples were activated by 1M HCl and quenched by 1M NaOH, following the manufacturer's instructions.

Quantitative RT-PCR

We isolated mRNA and performed qPCR as previously described (Shi et al. 2010). We quantified the expression of the following genes: thrombospondin-1 (Thbs1-001, RefSeq mRNA: NM_011580.3, forward primer: 5’-GCAAAGACTGTGTTGGCGATGTGA-3’, reverse primer: 5’-ACTCATCGACGTCTTTGCACTGGA-3’), iNOS (Nos2, RefSeq

mRNA: NM_010927.3, forward primer: 5'-TGACGGCAAACATGACTTCAG-3', reverse primer: 5'-GCCATCGGGCATCTGGTA-3'), fibronectin-1 (Fn1, RefSeq mRNA: NM_010233.1, forward primer: 5'-AGGCAATGGACGCATCAC-3', reverse primer: 5'-TTCCTCGGTTGTCCTTCTTG-3'), and tenascin-C (Tnc, RefSeq mRNA: NM_011607.3, forward primer: 5'-GCAACCAAGGACAATGTGTG-3', reverse primer: 5'-TGTGGTTTCAGACACCCGTA-3'). We used GAPDH as a control (Gapdh-001, RefSeq mRNA: NM_008084.2, forward primer: 5'-TGCACCACCAACTGCTTA G-3', reverse primer: 5'-GATGCAGGGATGATGTTC-3').

Behavioral scores

For the beam balance test (Manaenko et al. 2011) we used the following scoring system: 5 – mice move across the beam to their home cage in 6 seconds, 4 – mice move to their home cage in 11 seconds or in 6 seconds but do not get into the cage, 3 – mice move more than half the distance to their home cage within 11 seconds and stay on the beam for at least 6 seconds, 2 – mice do not move more than half the distance to their home cage within 11 seconds and stay on the beam for at least 6 seconds, 1 – mice do not move, but stay on the beam for 11 seconds, 0 – mice fall off the beam within 11 seconds. The Modified Garcia Score is a well-established sensorimotor assessment system consisting of 7 individual tests, of which we used the 5 that measure motor function (Doyle et al. 2012; Garcia et al. 1995). We scored each test from 0 to 3 (maximal score = 15): (1) climbing, (2) forelimb walking, (3) forelimb strength, (4) lateral turning, and (5) limb symmetry as described (Doyle et al. 2012).

Statistical analysis

All experimental data were acquired in a blinded and unbiased fashion. Statistical analyses were performed using Prism 6 software (GraphPad). Means between two groups were compared using two-tailed, unpaired Student's t test for parametric data, and Mann-Whitney test for non-parametric data. Means between more than two groups were compared using one-way ANOVA with Bonferroni correction for multiple comparisons. Comparisons of means from two genotypes at multiple timepoints were performed using two-way ANOVA when mouse cohorts were different at each timepoint, and repeated measures ANOVA when the same mice were used throughout the course of the experiment. For cluster analysis, cytokine detection in 80% of samples was used as a threshold, and the difference between clusters was computed based on Pearson's correlation.

Results

Construction of an "Ast-Tbr2DN" mouse model to inhibit astrocytic TGFβ signaling

To investigate astrocytic TGFβ signaling after stroke, we selected the model of distal middle cerebral artery occlusion (dMCAO) (Colak et al. 2011). The advantages of dMCAO are that it is directly caused by arterial occlusion and produces a highly consistent stroke with a clearly defined border. We previously reported that TGFβ signaling increases in $GFAP^+$ astrocytes in the peri-infarct cortex during the first week after dMCAO, as represented by nuclear localization of pSmad2 (Doyle et al. 2010)(Fig. 1A).

To study the function of endogenous astrocytic TGFβ signaling after stroke, we engineered a dominant negative (Ast-Tbr2DN) transgenic mouse model that inhibits TGFβ signaling specifically in $GFAP^+$ astrocytes (Fig. 1B). Adult Ast-Tbr2DN mice were indistinguishable from wildtypes prior to stroke based on gross anatomy, expression of GFAP, immune cell markers and cytokines, and motor function (data not shown). We verified that stroke upregulates the transgene specifically in $GFAP^+$ astrocytes by coimmunostaining for GFAP and the transgene marker eGFP. We observed that eGFP expression was present at baseline in approximately 10% of astrocytes. As expected, transgene expression significantly increased after dMCAO in the peri-infarct cortex (Fig. 1C). eGFP expression was completely specific to astrocytes at all timepoints and did not co-localize with any other cell types (Fig. 1D and data not shown).

To verify that the mutant TGFβ receptor was functional in reducing TGFβ signaling in $eGFP^+$ astrocytes in Ast-Tbr2DN mice, we immunostained for the downstream TGFβ signaling marker nuclear pSmad2 and quantified its colocalization with GFAP and with eGFP in the peri-infarct cortex. To avoid bias, we scored the co-localization of pSmad2 and GFAP prior to examining eGFP. Significantly fewer $GFAP^+/eGFP^+$ astrocytes in Ast-Tbr2DN mice co-localized with nuclear pSmad2 when compared to astrocytes in wildtype mice (Fig. 1E, 1F). By contrast, $GFAP^+/eGFP^-$ astrocytes in Ast-Tbr2DN mice showed the same proportion of nuclear pSmad2 as astrocytes in wildtype mice (Fig. 1F). Thus, in Ast-Tbr2DN mice the mutant type II TGFβ receptor blocks TGFβ signaling in $GFAP^+/eGFP^+$ astrocytes.

Inhibiting astrocytic TGFβ signaling increases the magnitude and spread of inflammation in the peri-infarct cortex

We next investigated whether normal astrocytic TGFβ signaling is required to limit neuroinflammation after stroke. Two days after stroke the immune response consists predominantly of activated monocytic cells, both CNS microglia and peripheral macrophages (Denker et al. 2007; Iadecola and Anrather 2011; Stevens et al. 2002). We used FACS to count activated microglia and macrophages in the stroked hemisphere of Ast-Tbr2DN mice and wildtype controls (Fig. 2A, 2B). $CD11b^+$ cells with medium CD45 expression were classified as activated CNS microglia, and $CD11b^+$ cells with high CD45 expression as peripheral macrophages (Mizutani et al. 2012). The stroked hemisphere of Ast-Tbr2DN mice contained significantly (67%) more cells in combined microglial and macrophage populations, with a particularly pronounced 110% increase in macrophages (Fig. 2B).

To assess whether inhibiting astrocytic TGFβ signaling affected the localization as well as the magnitude of the immune cell infiltration, we immunostained for CD68, which is a marker for activated microglia and macrophages. $CD68^+$ cells with activated amoeboid morphology were present in the peri-infarct cortex in both genotypes. We quantified the percentage of cortical area that was covered by CD68 immunostaining in a series of sections spanning the entire stroke region. In keeping with the flow cytometry results, the area covered by $CD68^+$ cells was 1.9-fold larger in Ast-Tbr2DN peri-infarct cortex as in wildtype controls (Fig. 2C, 2D).

To verify this increased spread of activated monocytic lineage cells, and to examine their activation state, we examined immunostaining for major histocompatibility complex class II (MHC II). MHC II regulates antigen presentation and is used as a marker for pro-inflammatory microglia and macrophages (Mantovani et al. 2004). As with the activated microglia and macrophage cell counts, and the CD68 immunostaining, we observed almost twice as many MHC II^+ cells in the peri-infarct cortex of Ast-Tbr2DN mice as in wildtype controls (Fig. 2E, 2F). Furthermore, MHC II^+ cells, like $CD68^+$ cells, appeared to be disseminated further from the infarct in Ast-Tbr2DN mice.

Activated microglia and macrophages also express inducible nitric oxide synthase (iNOS) (Kigerl et al. 2009; Mantovani et al. 2004) which leads to free radical formation and increases neuronal damage (Brown 2010). To assess whether inhibiting astrocytic TGFβ signaling increases iNOS expression after stroke, we used qPCR to measure iNOS mRNA levels in the peri-infarct cortex of Ast-Tbr2DN and wildtype mice (Fig. 2G). We observed 2-fold more iNOS mRNA in Ast-Tbr2DN than wildtype mice after stroke, which approximately correlates with the increased number of activated microglia and peripheral macrophages (Fig. 2B, 2D, 2F). These findings indicate that inhibiting astrocytic TGFβ signaling increases the magnitude and the extent of inflammation in the peri-infarct cortex as well as its potential neurotoxicity via iNOS production.

Inhibiting astrocytic TGFβ signaling does not affect initial stroke size or astrocytic activation in the peri-infarct cortex

One possible reason for a larger immune response in Ast-Tbr2DN mice could be a larger stroke. However, at this timepoint, 2 days after stroke, when we observed increased inflammation, stroke sizes were not different between genotypes (Fig. 3A).

A second possibility that could explain more immune cells in the brain after stroke might be an inadequate physical astrocytic barrier (Voskuhl et al. 2009; Wanner et al. 2013). However, we did not observe any morphological differences in $GFAP^+$ astrocytes between genotypes, including in the peri-infarct cortex. Furthermore, there were no genotype-dependent differences in % area covered by GFAP immunostaining in the peri-infarct cortex 3 days after stroke (Fig. 3B, 3C). Finally, we did not observe any differences between genotypes in GFAP immunostaining even after the immune response largely subsided, 7 days after stroke (wildtype: 12.59 ± 1.44%, Ast-Tbr2DN: 15.13 ± 2.23%, $P = 0.37$)

To perform a more thorough evaluation of early astrocyte activation and barrier formation, we also measured two extracellular matrix proteins that are upregulated in astrocytes during the subacute period after CNS injury (Schachtrup et al. 2010; Smith and Hale 1997; Zamanian et al. 2012): fibronectin-1 and tenascin C. As with GFAP, there was no difference in expression of either gene in Ast-Tbr2DN mice compared to wildtype controls (Fig. 3D, 3E). Thus, our results suggest astrocytic TGFβ signaling during the subacute period after stroke did not alter neuroinflammation by altering the astrocytic scar.

Astrocytic TGFβ signaling is required to upregulate the expression of TGF-β1 and its activator thrombospondin-1 in the peri-infarct cortex during the subacute period after stroke

Since astrocytes respond to CNS injury by producing cytokines and chemokines, we next investigated whether inhibiting astrocytic TGFβ signaling could increase inflammation by altering the cytokine milieu in the peri-infarct cortex. We measured a panel of 26 distinct pro- and anti-inflammatory cytokines and chemokines in the peri-infarct and contralateral cortex 2 days after stroke using a multiplex luminex assay. Three of these cytokines (IL-3, IL-10 and GCSF) were undetectable in the peri-infarct cortex.

Unbiased cluster analysis of the remaining 23 proteins revealed distinct patterns of expression based on genotype (Fig. 4A). However, TGF-β1 itself was the only cytokine that, on an individual basis, showed significant genotype-dependent differences, and thus it was the main factor that influenced sample clustering. There was a 3-fold reduction in TGF-β1 in the Ast-Tbr2DN peri-infarct cortex compared to wildtype (Fig. 4B), suggesting that inhibiting astrocytic TGFβ signaling disrupts a feed-forward mechanism by which TGFβ signaling in astrocytes normally propagates its own upregulation after stroke. We confirmed by ELISA that Ast-Tbr2DN mice have normal levels of TGF-β1 before stroke, but then fail to upregulate it normally in the peri-infarct cortex (Fig. 4C).

Of the 3 TGFβ isoforms, TGF-β1 is the one most upregulated by injury, including stroke in both animal models and human patients (Dhandapani and Brann 2003; Finch et al. 1993; Krupinski et al. 1996), though TGF-β2 can also be increased by stroke (Vivien and Ali 2006). To investigate whether TGFβ mRNA is upregulated by dMCAO, and whether astrocytic TGFβ signaling reduces its expression at mRNA level as well as protein level, we quantified the expression of TGF-β1, 2 and 3 mRNA by qPCR. We found that both TGF-β1 and TGF-β2, but not TGF-β3 mRNA in wildtype mice are significantly increased by two days after dMCAO (TGF-β1: 3.55 ± 0.70-fold, $*p = 0.011$; TGF-β2: 2.24 ± 0.26-fold, $**p = 0.0028$; TGF-β3: 0.92 ± 0.15-fold, $p = 0.82$, Student's t-test). However, we did not observe any differences between Ast-Tbr2DN mice and wildtype controls in either TGF-β1 or TGF-β2 mRNA expression (data not shown). In addition, TGF-β1 was the isoform that was most highly expressed after stroke, as its mRNA was expressed at 95.01 ± 1.22-fold higher level than TGF-β2 mRNA. Thus, astrocytic TGFβ signaling is required to induce TGF-β1 production primarily at the protein rather than the mRNA level.

After secretion TGF-β1 is stored in an inactive form in a latent complex that is bound to the extracellular matrix. This latent store of TGF-β1 requires activation in order to initiate TGFβ signaling (Annes et al. 2003). One major TGFβ activator is thrombospondin-1, which initiates protease-mediated cleavage of TGFβ from the latent complex and serves as the main TGFβ activator *in vivo* (Crawford et al. 1998). In addition, TGF-β1 is known to stimulate the production of thrombospondin-1 by astrocytes (Cambier et al. 2005; Yonezawa et al. 2010). Therefore, we investigated thrombospondin-1 as a potential astrocytic TGFβ-signaling dependent activator of TGF-β1 in the peri-infarct cortex.

We found that Ast-Tbr2DN mice fail to upregulate thrombospondin-1 mRNA 2 days after stroke, while wildtype mice upregulate it 5-fold (Fig. 4D). This finding suggests that after

stroke astrocytic TGFβ signaling participates in a positive feedback loop where it is required to upregulate both TGF-β1 and also its activator thrombospondin-1. There is one other TGFβ activator that is produced by astrocytes, integrin β8 (Cambier et al. 2005; Mu et al. 2002). However, we observed no significant difference in integrin β8 mRNA between Ast-Tbr2DN mice and wildtype controls 2 days after stroke (wildtype: 1.04 ± 0.155, Ast-Tbr2DN: 1.02 ± 0.148).

Ast-Tbr2DN mice exhibit a global reduction in TGFβ signaling after stroke

TGFβ signaling is upregulated subacutely in peri-infarct cortex in wildtype mice (Doyle et al. 2010). To evaluate whether the relative deficiency of TGF-β1 and thrombospondin-1 in Ast-Tbr2DN mice caused an overall reduction in downstream TGFβ signaling in the peri-infarct cortex, we examined Smad2 phosphorylation by Western blot. As with TGF-β1 protein levels, there was no difference before stroke (Fig. 5A, 5B). However, 2 days after stroke, Smad2 phosphorylation was significantly reduced in the Ast-Tbr2DN peri-infarct cortex (Fig. 5C, 5D), consistent with a decrease in TGF-β1 and its activator thrombospondin-1. By seven days after stroke, thrombospondin-1 mRNA in Ast-Tbr2DN mice reached wildtype levels (normalized WT: 1.00 ± 0.23, Ast-Tbr2DN: 1.36 ± 0.27, P = 0.35). At this later timepoint, Smad2 phosphorylation also returned to normal (normalized WT: 1.00 ± 0.05, Ast-Tbr2DN: 0.87 ± 0.09, P = 0.25). Thus, the primary effect of astrocytic TGFβ signaling on these parameters was on the subacute upregulation of TGFβ signaling after stroke.

To assess whether this overall decrease in subacute TGFβ signaling meant that there was a global effect throughout the peri-infarct region (i.e., an effect on TGFβ pathway activation in non-astrocyte cell types), we examined Akt pathway activation in neurons. We selected Akt phosphorylation because it is neuroprotective after ischemia and a neuronal target of TGFβ signaling after stroke (Zhao et al. 2006; Zhu et al. 2004). Indeed, Western blots for phosphorylated and total Akt indicated an overall decrease in Akt phosphorylation in the peri-infarct cortex of Ast-Tbr2DN mice 2 days after stroke compared to controls (Fig. 5E, 5F). We next immunostained for pAkt 2 days after stroke and found that pAkt was primarily, although not exclusively, neuronal. It co-localized with the neuronal nuclear marker NeuN, and immunostaining was decreased throughout the peri-infarct cortex in Ast-Tbr2DN mice (Fig. 5G). Furthermore, when we quantified the percent of neurons that exhibited any nuclear pAkt immunostaining, there were significantly fewer $pAkt^{+}/NeuN^{+}$ nuclei in Ast-Tbr2DN mice than in WT mice (Fig. 5H). Thus, the relative deficiency in TGFβ signaling after stroke in Ast-Tbr2DN mice causes decreased TGFβ signaling in neurons as well as in astrocytes.

Inhibiting astrocytic TGFβ signaling worsens motor outcomes during the first week after stroke

The dMCAO stroke model does not produce motor deficits, so to investigate whether increased inflammation and neuronal damage in Ast-Tbr2DN mice is physiologically important for motor recovery, we targeted the motor cortex using the photothrombotic stroke model. As with dMCAO, there was no difference in infarct sizes early after stroke (Fig. 6A).

However, by 4 weeks we observed 1.5-fold larger strokes in Ast-Tbr2DN mice than in wildtype controls (Fig. 6B).

To test motor outcomes, we subjected Ast-Tbr2DN mice and wildtype controls to the beam balance test as well as to a battery of motor tests, which are collectively known as the modified Garcia test, weekly for 4 weeks following photothrombotic stroke. Neither wildtype nor Ast-Tbr2DN mice showed any behavioral impairment at baseline.

In the beam balance test, Ast-Tbr2DN mice performed significantly worse during the first week after stroke (Fig. 6C), though both genotypes achieved full recovery by four weeks. By comparison, neither genotype demonstrated full motor recovery in the modified Garcia test by 4 weeks after stroke. In this test Ast-Tbr2DN mice exhibited a larger motor deficit within the first week after stroke that persisted throughout the testing (Fig. 6D - 6H). This deficit in Ast-Tbr2DN mice appeared as a trend in subtests of limb symmetry, forelimb strength and lateral turning (Fig. 6D - 6F) and was highly significant in forelimb walking and climbing (Fig. 6G, 6H). Overall, the combined motor test score indicated significantly worse motor outcomes in Ast-Tbr2DN mice (Fig. 6I). Together, these results show that astrocytic TGFβ signaling limits both infarct expansion and the severity of motor deficits.

Discussion

We demonstrate here that astrocytic TGFβ signaling functions to limit immune cell infiltration and activation after stroke. Interestingly, the immunoregulatory effects of astrocytic TGFβ signaling are a distinct mechanism, independent of the physical barrier formed by astrocytes: we observed no differences in the expression of GFAP and ECM components between mice with normal and reduced astrocytic TGFβ signaling. Instead, our results are consistent with a model in which TGFβ signaling in astrocytes upregulates beneficial TGFβ signaling in the peri-infarct cortex during the subacute time window after stroke by upregulating the expression of TGF-β1 and its activator thrombospondin-1 (Fig. 7). This positive feedback loop then limits neuroinflammation and neuronal injury in the peri-infarct cortex via the immunosuppressive and neuroprotective functions of TGFβ.

We found that that astrocytic TGFβ signaling limits the magnitude and spread of the immune response to stroke, but found no evidence that it affected immune cell polarization. Ast-Tbr2DN mice with reduced astrocytic TGFβ signaling exhibited a 2-fold increase in the number of activated microglia and macrophages 2 days after stroke. We next quantified two markers of pro-inflammatory macrophages and microglia, MHC II and iNOS, and observed a corresponding 2-fold upregulation, consistent with twice as many cells rather than a change in immune cell phenotype. In addition, since Ast-Tbr2DN and wildtype stroke volumes were not significantly different at this time point, this excessive neuroinflammation was not caused by a difference in stroke size.

Excessive neuroinflammation in Ast-Tbr2DN mice was however associated with increased neuronal dysfunction and injury, represented by impaired motor recovery and late infarct expansion in the photothrombotic stroke model. The photothrombotic stroke model was used not only to measure motor outcomes but also to increase accuracy in measuring late

infarct size because it produces a much larger stroke than the dMCAO model. In contrast, dMCAO in C57BL/6J mice does not produce a motor deficit, and the infarct cannot be easily measured by 4 weeks after stroke due to cortical atrophy. However, neither dMCAO nor photothrombotic stroke sizes were different between genotypes 1 day after infarction, before the peak immune response.

Neuronal dysfunction in Ast-Tbr2DN mice may have occurred secondary to the 2-fold increase in iNOS, which is known to be neurotoxic by stimulating free radical production (Brown 2010). In addition, both TGFβ and TGFβ pathway activation were also significantly lower in Ast-Tbr2DN peri-infarct cortex 2 days after stroke. TGFβ is well known to be directly anti-apoptotic and neuroprotective following stroke (Pang et al. 2001; Ruocco et al. 1999), in part by activating the PI3K/Akt pathway that leads to Akt phosphorylation in neurons (Zhu et al. 2004; Zhu et al. 2002). Indeed, we did observe a lower probability of nuclear pAkt immunostaining in Ast-Tbr2DN mouse neurons after stroke and an overall reduction in pAkt in peri-infarct cortex. Thus, when TGFβ signaling is normally upregulated in wildtype mice in the subacute period after stroke it may provide neuroprotection against secondary injury in the peri-infarct cortex. However, it is important to note that TGFβ signaling involves multiple pathways in addition to the classic canonical pathways mediated by Smads. The Akt pathway is only one of the non-canonical signaling pathways activated by TGFβ. Other non-canonical pathways that it activates, such as MAPK and Erk mediated signaling (Zhang 2009), could also potentially affect TGFβ-induced neuroprotection after stroke.

This study is, to our knowledge, the first time that an astrocytic signaling pathway has been shown to limit neuroinflammation without affecting the physical barrier formed by astrocytes. Either ablating proliferating $GFAP^+$ astrocytes or deleting the inflammatory mediator STAT3 in astrocytes reduces the physical barrier and increases immune cell infiltration after traumatic brain and spinal cord injuries (Bush et al. 1999; Wanner et al. 2013). Similarly, expressing a dominant negative inhibitor of pro-inflammatory NF-κB signaling both increases astrocytic scarring and reduces the expression of pro-inflammatory cytokines after spinal cord injury and ischemia (Brambilla et al. 2005; Dvoriantchikova et al. 2009). In contrast, here we found that when astrocytic TGFβ signaling is inhibited, there is more immune cell infiltration without changes in the expression of GFAP or two other components of the physical barrier, tenascin-C and fibronectin.

Although inhibiting astrocytic TGFβ signaling did not change the physical barrier formed by astrocytes, we did observe that it significantly altered cytokine expression in the peri-infarct cortex. Astrocytes with reduced TGFβ signaling were unable to stimulate the expression of the injury-responsive TGFβ isoform TGF-β1 and its activator thrombospondin-1 in the subacute time window after stroke. Interestingly, thrombospondin-1 has not previously been implicated in TGFβ activation after stroke.

While our findings cannot exclude the existence of other TGFβ activating molecules that are affected by astrocytic TGFβ-signaling after stroke, thrombospondin-1 is known to be a major activator of TGFβ *in vivo* (Crawford et al. 1998), and TGFβ is known to induce thrombospondin-1 transcription in astrocytes (Ikeda et al. 2010).

Thus, our results indicate that instead of altering the physical barrier formed by astrocytes, TGFβ signaling affects what the astrocytes secrete. We therefore speculate that in addition to their ability to generate a physical barrier, astrocytes form a "secretory" barrier to injury, composed at least in part by molecules such as TGFβ that astrocytes secrete to limit neuroinflammation.

Our results further reveal that normal astrocytic TGFβ signaling regulates this secretory barrier in a time and location-specific manner: inhibiting astrocytic TGFβ signaling primarily affected the levels of active TGFβ during the subacute time period and in the peri-infarct cortex. This subacute time window was also the critical time period in which TGFβ signaling in $GFAP^+$ astrocytes was required to limit inflammation. By comparison, inhibiting astrocytic TGFβ signaling had no effect on inflammatory cells or cytokines, astrocyte activation, or motor performance at baseline. Similarly, we did not observe any differences between genotypes on or after 7 days after stroke either in neuroinflammation or in worsening of the behavioral deficit. Thrombospondin-1 expression also returned to wildtype levels by 7 days, potentially because sufficient thrombospondin-1 was produced by activated microglia and macrophages (Lanz et al. 2010; Ortiz-Masia et al. 2012). This temporal specificity suggests a clinically relevant time window to target astrocytic TGFβ signaling for maximal benefit.

In the context of previous studies on global differences in TGFβ levels after injury, it was surprising that decreased astrocytic TGFβ signaling did not reduce GFAP expression and alter the astrocytic scar after stroke. TGF-β1 directly stimulates astrocytic expression of GFAP (Reilly et al. 1998; Romao et al. 2008) as well as the ECM components fibronectin and tenascin-C (Schachtrup et al. 2010; Smith and Hale 1997). In addition, mice that overexpress mutant, constitutively active TGF-β1 in the hippocampus have increased GFAP expression (Wyss-Coray et al. 1997), while global depletion of TGFβ reduces GFAP expression after traumatic brain injury (Logan et al. 1994; Yoshioka et al. 2011). By contrast, we show that inhibiting endogenous astrocytic TGFβ signaling and global TGFβ upregulation did not affect the expression of these physical barrier components. This incongruity could be caused by differences in TGFβ activation between injury models, or because global TGFβ signaling in our model was partially rather than completely inhibited. Alternatively, increased immune infiltration in Ast-Tbr2DN mice early after stroke could increase GFAP expression via another pathway, for example, NF-κB signaling (Gao et al. 2013; Krohn et al. 1999), which would compensate for reduced GFAP expression caused by reduced astrocytic TGFβ signaling.

In conclusion, we demonstrate that inhibiting endogenous astrocytic TGFβ signaling during the subacute period after stroke prevents the upregulation of functional TGFβ and its signaling in the peri-infarct cortex and strongly exacerbates infiltration and activation of innate immune cells. Since TGFβ is upregulated universally in acute and chronic brain injury, it may represent a universal pathway that mediates the endogenous immunoregulatory functions of astrocytes. The anti-inflammatory and pro-recovery functions of astrocytic TGFβ signaling may therefore extend to other acute insults, such as traumatic brain injury or CNS infection, which are also characterized by increased TGF-β1 (Buckwalter and Wyss-Coray 2004).

Acknowledgments

The authors would like to thank Dr. Yael Rosenberg-Hasson of the Stanford Human Immune Monitoring Center, Bianca Gomez of the Stanford Shared FACS Facility and Dr. Andrew Olson of the Stanford Neuroscience Microscopy Services for technical assistance with data collection. We thank Drs. Anita Koshy, Brenda Porter and Katrin Andreasson for critical review of the manuscript. Funding sources: AHA 10GRNT4140073 (MSB) and NINDS R01067132 (MSB), AHA 11PRE6970002 (EC) and Stanford Graduate Fellowship (EC).

Bibliography

Annes JP, Munger JS, Rifkin DB. Making sense of latent TGFbeta activation. J Cell Sci. 2003; 116:217–24. [PubMed: 12482908]

Arac A, Brownell SE, Rothbard JB, Chen C, Ko RM, Pereira MP, Albers GW, Steinman L, Steinberg GK. Systemic augmentation of alphaB-crystallin provides therapeutic benefit twelve hours post-stroke onset via immune modulation. Proceedings of the National Academy of Sciences of the United States of America. 2011; 108:13287–92. [PubMed: 21828004]

Babcock AA, Kuziel WA, Rivest S, Owens T. Chemokine expression by glial cells directs leukocytes to sites of axonal injury in the CNS. J Neurosci. 2003; 23:7922–30. [PubMed: 12944523]

Barreto G, White RE, Ouyang Y, Xu L, Giffard RG. Astrocytes: targets for neuroprotection in stroke. Cent Nerv Syst Agents Med Chem. 2011; 11:164–73. [PubMed: 21521168]

Brambilla R, Bracchi-Ricard V, Hu WH, Frydel B, Bramwell A, Karmally S, Green EJ, Bethea JR. Inhibition of astroglial nuclear factor kappaB reduces inflammation and improves functional recovery after spinal cord injury. The Journal of experimental medicine. 2005; 202:145–56. [PubMed: 15998793]

Brenner M, Kisseberth WC, Su Y, Besnard F, Messing A. GFAP promoter directs astrocyte-specific expression in transgenic mice. J Neurosci. 1994; 14:1030–7. [PubMed: 8120611]

Brown GC. Nitric oxide and neuronal death. Nitric Oxide. 2010; 23:153–65. [PubMed: 20547235]

Buckwalter M, Wyss-Coray T. Modelling neuroinflammatory phenotypes in vivo. J Neuroinflammation. 2004; 1:10. [PubMed: 15285805]

Bush TG, Puvanachandra N, Horner CH, Polito A, Ostenfeld T, Svendsen CN, Mucke L, Johnson MH, Sofroniew MV. Leukocyte infiltration, neuronal degeneration, and neurite outgrowth after ablation of scar-forming, reactive astrocytes in adult transgenic mice. Neuron. 1999; 23:297–308. [PubMed: 10399936]

Cambier S, Gline S, Mu D, Collins R, Araya J, Dolganov G, Einheber S, Boudreau N, Nishimura SL. Integrin alpha(v)beta8-mediated activation of transforming growth factor-beta by perivascular astrocytes: an angiogenic control switch. Am J Pathol. 2005; 166:1883–94. [PubMed: 15920172]

Chen Y, Swanson RA. Astrocytes and brain injury. J Cereb Blood Flow Metab. 2003; 23:137–49. [PubMed: 12571445]

Clarkson AN, Overman JJ, Zhong S, Mueller R, Lynch G, Carmichael ST. AMPA receptor-induced local brain-derived neurotrophic factor signaling mediates motor recovery after stroke. J Neurosci. 2011; 31:3766–75. [PubMed: 21389231]

Colak G, Filiano AJ, Johnson GV. The application of permanent middle cerebral artery ligation in the mouse. J Vis Exp. 2011

Crawford SE, Stellmach V, Murphy-Ullrich JE, Ribeiro SMF, Lawler J, Hynes RO, Boivin GP, Bouck N. Thrombospondin-1 is a major activator of TGF-b1 in vivo. Cell. 1998; 93:1159–1170. [PubMed: 9657149]

Crowe MJ, Doetschman T, Greenhalgh DG. Delayed wound healing in immunodeficient TGF-beta 1 knockout mice. J Invest Dermatol. 2000; 115:3–11. [PubMed: 10886500]

Denker SP, Ji S, Dingman A, Lee SY, Derugin N, Wendland MF, Vexler ZS. Macrophages are comprised of resident brain microglia not infiltrating peripheral monocytes acutely after neonatal stroke. J Neurochem. 2007; 100:893–904. [PubMed: 17212701]

Dhandapani KM, Brann DW. Transforming growth factor-beta: a neuroprotective factor in cerebral ischemia. Cell Biochem Biophys. 2003; 39:13–22. [PubMed: 12835526]

Dheen ST, Kaur C, Ling EA. Microglial activation and its implications in the brain diseases. Curr Med Chem. 2007; 14:1189–97. [PubMed: 17504139]

Doyle KP, Cekanaviciute E, Mamer LE, Buckwalter MS. TGFbeta signaling in the brain increases with aging and signals to astrocytes and innate immune cells in the weeks after stroke. Journal of neuroinflammation. 2010; 7:62. [PubMed: 20937129]

Doyle KP, Fathali N, Siddiqui MR, Buckwalter MS. Distal hypoxic stroke: a new mouse model of stroke with high throughput, low variability and a quantifiable functional deficit. J Neurosci Methods. 2012; 207:31–40. [PubMed: 22465679]

Dvoriantchikova G, Barakat D, Brambilla R, Agudelo C, Hernandez E, Bethea JR, Shestopalov VI, Ivanov D. Inactivation of astroglial NF-kappa B promotes survival of retinal neurons following ischemic injury. Eur J Neurosci. 2009; 30:175–85. [PubMed: 19614983]

Fadok VA, Bratton DL, Konowal A, Freed PW, Westcott JY, Henson PM. Macrophages that have ingested apoptotic cells in vitro inhibit proinflammatory cytokine production through autocrine/paracrine mechanisms involving TGF-b, PGE2, and PAF. J Clin Invest. 1998; 101:890–898. [PubMed: 9466984]

Finch CE, Laping NJ, Morgan TE, Nichols NR, Pasinetti GM. TGF-b1 is an organizer of responses to neurodegeneration. J Cell Biochem. 1993; 53:314–322. [PubMed: 8300749]

Florian C, Vecsey CG, Halassa MM, Haydon PG, Abel T. Astrocyte-derived adenosine and A1 receptor activity contribute to sleep loss-induced deficits in hippocampal synaptic plasticity and memory in mice. J Neurosci. 2011; 31:6956–62. [PubMed: 21562257]

Frugier T, Koishi K, Matthaei KI, McLennan IS. Transgenic mice carrying a tetracycline-inducible, truncated transforming growth factor beta receptor (TbetaRII). Genesis. 2005; 42:1–5. [PubMed: 15828000]

Gao Z, Zhu Q, Zhang Y, Zhao Y, Cai L, Shields CB, Cai J. Reciprocal Modulation Between Microglia and Astrocyte in Reactive Gliosis Following the CNS Injury. Mol Neurobiol. 2013

Garcia JH, Wagner S, Liu KF, Hu XJ. Neurological deficit and extent of neuronal necrosis attributable to middle cerebral artery occlusion in rats. Statistical validation. Stroke. 1995; 26:627–34. discussion 635. [PubMed: 7709410]

Glabinski AR, Balasingam V, Tani M, Kunkel SL, Strieter RM, Yong VW, Ransohoff RM. Chemokine monocyte chemoattractant protein-1 is expressed by astrocytes after mechanical injury to the brain. J Immunol. 1996; 156:4363–8. [PubMed: 8666808]

Halassa MM, Florian C, Fellin T, Munoz JR, Lee SY, Abel T, Haydon PG, Frank MG. Astrocytic modulation of sleep homeostasis and cognitive consequences of sleep loss. Neuron. 2009; 61:213–9. [PubMed: 19186164]

Heiss WD. The ischemic penumbra: how does tissue injury evolve? Ann N Y Acad Sci. 2012; 1268:26–34. [PubMed: 22994218]

Iadecola C, Anrather J. The immunology of stroke: from mechanisms to translation. Nature medicine. 2011; 17:796–808.

Ikeda H, Miyatake M, Koshikawa N, Ochiai K, Yamada K, Kiss A, Donlin MJ, Panneton WM, Churchill JD, Green M. Morphine modulation of thrombospondin levels in astrocytes and its implications for neurite outgrowth and synapse formation. J Biol Chem. Others;2010 285:38415–27. [PubMed: 20889977]

Kigerl KA, Gensel JC, Ankeny DP, Alexander JK, Donnelly DJ, Popovich PG. Identification of two distinct macrophage subsets with divergent effects causing either neurotoxicity or regeneration in the injured mouse spinal cord. J Neurosci. 2009; 29:13435–44. [PubMed: 19864556]

Krohn K, Rozovsky I, Wals P, Teter B, Anderson CP, Finch CE. Glial fibrillary acidic protein transcription responses to transforming growth factor-beta1 and interleukin-1beta are mediated by a nuclear factor-1-like site in the near-upstream promoter. J Neurochem. 1999; 72:1353–61. [PubMed: 10098836]

Krupinski J, Kumar P, Kumar S, Kaluza J. Increased expression of TGF-b1 in brain tissue after ischemic stroke in humans. Stroke. 1996; 27:852–857. [PubMed: 8623105]

Lanz TV, Ding Z, Ho PP, Luo J, Agrawal AN, Srinagesh H, Axtell R, Zhang H, Platten M, Wyss-Coray T. Angiotensin II sustains brain inflammation in mice via TGF-beta. J Clin Invest. 2010; 120:2782–94. others. [PubMed: 20628203]

Li L, Lundkvist A, Andersson D, Wilhelmsson U, Nagai N, Pardo AC, Nodin C, Stahlberg A, Aprico K, Larsson K. Protective role of reactive astrocytes in brain ischemia. Journal of cerebral blood flow and metabolism : official journal of the International Society of Cerebral Blood Flow and Metabolism. 2008; 28:468–81. others.

Lin HY, Yang LT. Differential response of epithelial stem cell populations in hair follicles to TGF-beta signaling. Dev Biol. 2013; 373:394–406. [PubMed: 23103542]

Logan A, Berry M, Gonzalez A, Frautschy S, Sporn M, Baird A. Effects of transforming growth factor beta 1 on scar production in the injured central nervous systems of the rat. Eur J Neurosci. 1994; 6:355–363. [PubMed: 8019673]

Manaenko A, Fathali N, Khatibi NH, Lekic T, Hasegawa Y, Martin R, Tang J, Zhang JH. Arginine-vasopressin V1a receptor inhibition improves neurologic outcomes following an intracerebral hemorrhagic brain injury. Neurochem Int. 2011; 58:542–8. [PubMed: 21256175]

Mantovani A, Sica A, Sozzani S, Allavena P, Vecchi A, Locati M. The chemokine system in diverse forms of macrophage activation and polarization. Trends in immunology. 2004; 25:677–86. [PubMed: 15530839]

Massagué J, Wotton D. Transcriptional control by the TGF-b/Smad signaling system. EMBO J. 2000; 19:1745–1754. [PubMed: 10775259]

Mizutani M, Pino PA, Saederup N, Charo IF, Ransohoff RM, Cardona AE. The fractalkine receptor but not CCR2 is present on microglia from embryonic development throughout adulthood. J Immunol. 2012; 188:29–36. [PubMed: 22079990]

Mu D, Cambier S, Fjellbirkeland L, Baron JL, Munger JS, Kawakatsu H, Sheppard D, Broaddus VC, Nishimura SL. The integrin alpha(v)beta8 mediates epithelial homeostasis through MT1-MMP-dependent activation of TGF-beta1. J Cell Biol. 2002; 157:493–507. [PubMed: 11970960]

Ortiz-Masia D, Diez I, Calatayud S, Hernandez C, Cosin-Roger J, Hinojosa J, Esplugues JV, Barrachina MD. Induction of CD36 and thrombospondin-1 in macrophages by hypoxia-inducible factor 1 and its relevance in the inflammatory process. PLoS One. 2012; 7:e48535. [PubMed: 23119050]

Pang L, Ye W, Che XM, Roessler BJ, Betz AL, Yang GY. Reduction of Inflammatory Response in the Mouse Brain With Adenoviral-Mediated Transforming Growth Factor-1 Expression. Stroke; a journal of cerebral circulation. 2001; 32:544–552.

Pascual O, Casper KB, Kubera C, Zhang J, Revilla-Sanchez R, Sul JY, Takano H, Moss SJ, McCarthy K, Haydon PG. Astrocytic purinergic signaling coordinates synaptic networks. Science. 2005; 310:113–6. [PubMed: 16210541]

Pineau I, Sun L, Bastien D, Lacroix S. Astrocytes initiate inflammation in the injured mouse spinal cord by promoting the entry of neutrophils and inflammatory monocytes in an IL-1 receptor/MyD88-dependent fashion. Brain Behav Immun. 2010; 24:540–53. [PubMed: 19932745]

Pratt BM, McPherson JM. TGF-beta in the central nervous system: potential roles in ischemic injury and neurodegenerative diseases. Cytokine Growth Factor Rev. 1997; 8:267–92. [PubMed: 9620642]

Rani R, Smulian AG, Greaves DR, Hogan SP, Herbert DR. TGF-beta limits IL-33 production and promotes the resolution of colitis through regulation of macrophage function. Eur J Immunol. 2011; 41:2000–9. [PubMed: 21469118]

Reilly JF, Maher PA, Kumari VG. Regulation of astrocyte GFAP expression by TGF-beta1 and FGF-2. Glia. 1998; 22:202–10. [PubMed: 9537840]

Romao LF, Sousa Vde O, Neto VM, Gomes FC. Glutamate activates GFAP gene promoter from cultured astrocytes through TGF-beta1 pathways. J Neurochem. 2008; 106:746–56. [PubMed: 18419760]

Ruocco A, Nicole O, Docagne F, Ali C, Chazalviel L, Komesli S, Yablonsky F, Roussel S, MacKenzie ET, Vivien D. A transforming growth factor-beta antagonist unmasks the neuroprotective role of this endogenous cytokine in excitotoxic and ischemic brain injury. Journal of cerebral blood flow and metabolism : official journal of the International Society of Cerebral Blood Flow and Metabolism. 1999; 19:1345–53. others.

Schachtrup C, Ryu JK, Helmrick MJ, Vagena E, Galanakis DK, Degen JL, Margolis RU, Akassoglou K. Fibrinogen triggers astrocyte scar formation by promoting the availability of active TGF-beta after vascular damage. J Neurosci. 2010; 30:5843–54. [PubMed: 20427645]

Shi J, Johansson J, Woodling NS, Wang Q, Montine TJ, Andreasson K. The prostaglandin E2 E-prostanoid 4 receptor exerts anti-inflammatory effects in brain innate immunity. J Immunol. 2010; 184:7207–18. [PubMed: 20483760]

Shi Y, Massague J. Mechanisms of TGF-beta signaling from cell membrane to the nucleus. Cell. 2003; 113:685–700. [PubMed: 12809600]

Smith GM, Hale JH. Macrophage/Microglia regulation of astrocytic tenascin: synergistic action of transforming growth factor-beta and basic fibroblast growth factor. J Neurosci. 1997; 17:9624–33. [PubMed: 9391017]

Sofroniew MV, Vinters HV. Astrocytes: biology and pathology. Acta Neuropathol. 2010; 119:7–35. [PubMed: 20012068]

Stevens SL, Bao J, Hollis J, Lessov NS, Clark WM, Stenzel-Poore MP. The use of flow cytometry to evaluate temporal changes in inflammatory cells following focal cerebral ischemia in mice. Brain Res. 2002; 932:110–9. [PubMed: 11911867]

Vivien D, Ali C. Transforming growth factor-beta signalling in brain disorders. Cytokine & growth factor reviews. 2006; 17:121–8. [PubMed: 16271500]

Voskuhl RR, Peterson RS, Song B, Ao Y, Morales LB, Tiwari-Woodruff S, Sofroniew MV. Reactive astrocytes form scar-like perivascular barriers to leukocytes during adaptive immune inflammation of the CNS. J Neurosci. 2009; 29:11511–22. [PubMed: 19759299]

Wanner IB, Anderson MA, Song B, Levine J, Fernandez A, Gray-Thompson Z, Ao Y, Sofroniew MV. Glial Scar Borders Are Formed by Newly Proliferated, Elongated Astrocytes That Interact to Corral Inflammatory and Fibrotic Cells via STAT3-Dependent Mechanisms after Spinal Cord Injury. J Neurosci. 2013; 33:12870–86. [PubMed: 23904622]

Woo MS, Wang X, Faustino JV, Derugin N, Wendland MF, Zhou P, Iadecola C, Vexler ZS. Genetic deletion of CD36 enhances injury after acute neonatal stroke. Ann Neurol. 2012; 72:961–70. [PubMed: 23280844]

Wyss-Coray T, Borrow P, Brooker MJ, Mucke L. Astroglial overproduction of TGF-beta 1 enhances inflammatory central nervous system disease in transgenic mice. Journal of neuroimmunology. 1997; 77:45–50. [PubMed: 9209267]

Yamashita K, Gerken U, Vogel P, Hossmann K, Wiessner C. Biphasic expression of TGF-beta1 mRNA in the rat brain following permanent occlusion of the middle cerebral artery. Brain Res. 1999; 836:139–45. [PubMed: 10415412]

Yonezawa T, Hattori S, Inagaki J, Kurosaki M, Takigawa T, Hirohata S, Miyoshi T, Ninomiya Y. Type IV collagen induces expression of thrombospondin-1 that is mediated by integrin alpha1beta1 in astrocytes. Glia. 2010; 58:755–67. [PubMed: 20091789]

Yoshioka N, Kimura-Kuroda J, Saito T, Kawamura K, Hisanaga S, Kawano H. Small molecule inhibitor of type I transforming growth factor-beta receptor kinase ameliorates the inhibitory milieu in injured brain and promotes regeneration of nigrostriatal dopaminergic axons. J Neurosci Res. 2011; 89:381–93. [PubMed: 21259325]

Zamanian JL, Xu L, Foo LC, Nouri N, Zhou L, Giffard RG, Barres BA. Genomic analysis of reactive astrogliosis. J Neurosci. 2012; 32:6391–410. [PubMed: 22553043]

Zhang YE. Non-Smad pathways in TGF-beta signaling. Cell Res. 2009; 19:128–39. [PubMed: 19114990]

Zhao H, Sapolsky RM, Steinberg GK. Phosphoinositide-3-kinase/akt survival signal pathways are implicated in neuronal survival after stroke. Mol Neurobiol. 2006; 34:249–70. [PubMed: 17308356]

Zhu Y, Culmsee C, Klumpp S, Krieglstein J. Neuroprotection by transforming growth factor-beta1 involves activation of nuclear factor-kappaB through phosphatidylinositol-3-OH kinase/Akt and mitogen-activated protein kinaseextracellular-signal regulated kinase1,2 signaling pathways. Neuroscience. 2004; 123:897–906. [PubMed: 14751283]

Zhu Y, Yang G-Y, Ahlemeyer B, Pang L, Che X-M, Culmsee C, Klumpp S, Krieglstein J. Transforming growth factor-b1 increases bad phosphorylation and protects neurons against damage. J Neurosci. 2002; 22:3898–3909. [PubMed: 12019309]

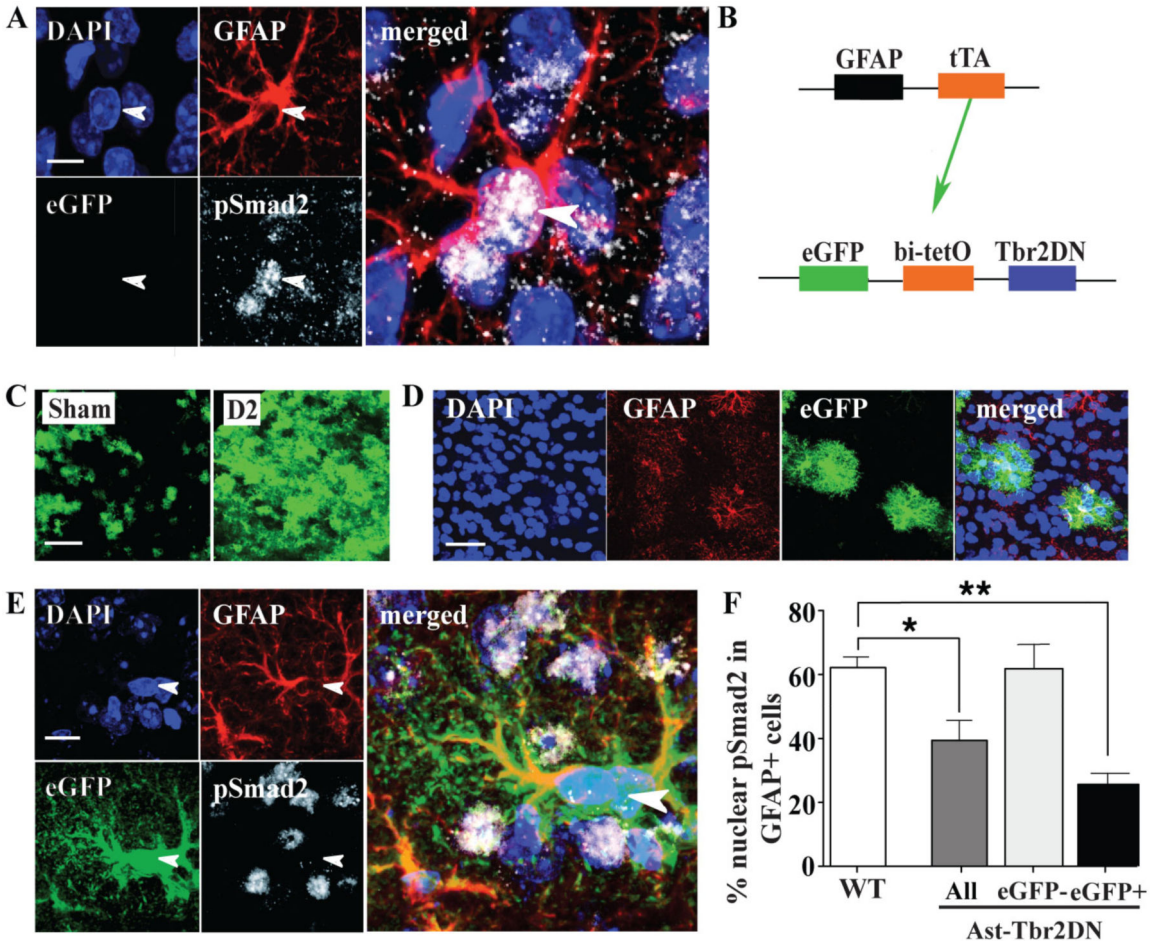

Figure 1. TGFβ signaling is specifically inhibited in astrocytes in Ast-Tbr2DN mice

A. Representative images of the TGFβ pathway activation marker pSmad2 co-localized with a GFAP$^+$ cell nucleus in the peri-infarct cortex of a wildtype mouse 24 hours after dMCAO. Note that astrocytes are not the only cell types responding to TGFβ. Arrow, a GFAP$^+$ cell expressing pSmad2 after dMCAO. Scale bar, 20 μm. **B.** Diagram of the Ast-Tbr2DN mouse model. The tetracycline transactivator protein (tTA) is driven by a GFAP promoter. tTA then binds the bidirectional bi-tetO promoter to drive two genes, eGFP and the dominant negative mutant type II TGFβ receptor, Ast-Tbr2DN-Tbr2. **C.** Representative images of eGFP expression in Ast-Tbr2DN mice in uninjured cortex (sham) and in the peri-infarct cortex 2 days after dMCAO (D2). Scale bar, 200 μm. **D.** Representative images showing specific eGFP expression in GFAP$^+$ cells in Ast-Tbr2DN mice. Scale bar, 50 μm. **E, F.** eGFP$^+$ astrocytes in Ast-Tbr2DN mice are less likely to demonstrate nuclear expression of pSmad2 than controls 24 hours after dMCAO. Representative images (**E**) and quantification (**F**). Arrow, a typical GFAP$^+$/eGFP$^+$ cell that does not express nuclear pSmad2. Scale bar, 20 μm. N=4 mice per group, 100 GFAP$^+$ cells per mouse. Bars, mean ± SEM. *P<0.05, **P<0.01, 1-way ANOVA, Bonferroni correction to compare with sham or wildtype.

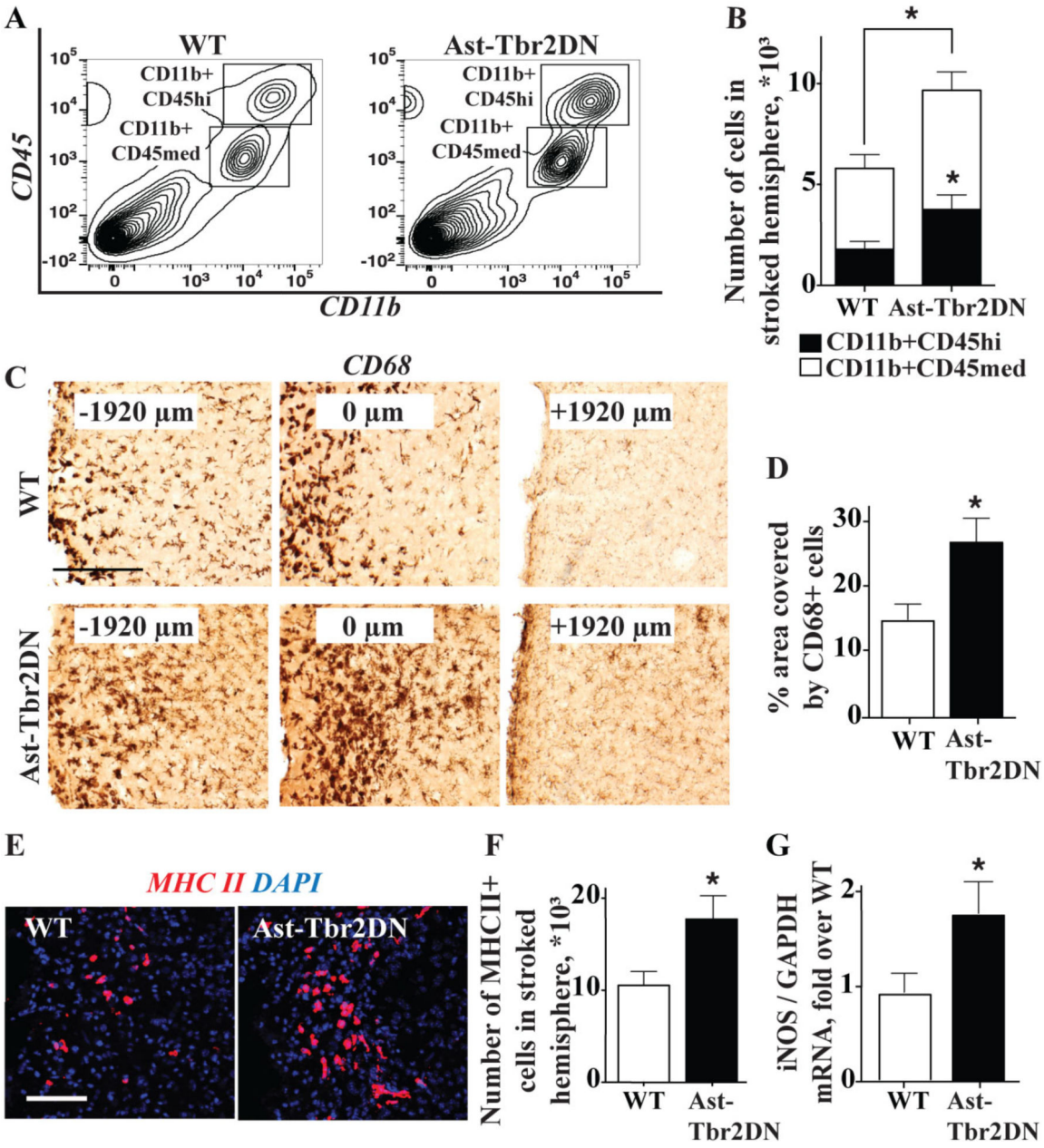

Figure 2. Inhibiting astrocytic TGFβ signaling increases inflammation in the peri-infarct cortex during the subacute period after dMCAO

A, B. Representative flow cytometry plots (**A**) and quantification (**B**) of $CD11b^+$ CD45 medium and $CD11b^+$ CD45 high monocytes in the peri-infarct cortex of Ast-Tbr2DN mice and wildtype controls. **C.** Representative images of CD68 immunostaining along the rostral-caudal axis across the peri-infarct cortex 3 days after dMCAO. The coronal section showing the largest stroke was arbitrarily designated as 0 µm, and $CD68^+$ cell activation was more prominent in Ast-Tbr2DN mice both rostral (-1920 µm) and caudal to that location (+1920 µm) Scale bar, 200µm. **D.** Quantification of CD68 immunostaining 3 days after dMCAO in the peri-infarct cortex, extending 1920 µm rostral and caudal from the section with maximal stroke size, demonstrates much more extensive spread of CD68 activation in Ast-Tbr2DN

mice. **E, F.** Representative images (**E**) and quantification (**F**) of MHC II immunostaining in the peri-infarct cortex 3 days after dMCAO. Scale bar, 100μm. **G.** Quantification of iNOS mRNA in Ast-Tbr2DN mice and wildtype controls. N=6-12 mice per group. Bars, mean ± SEM. **P*<0.05, Student's t test.

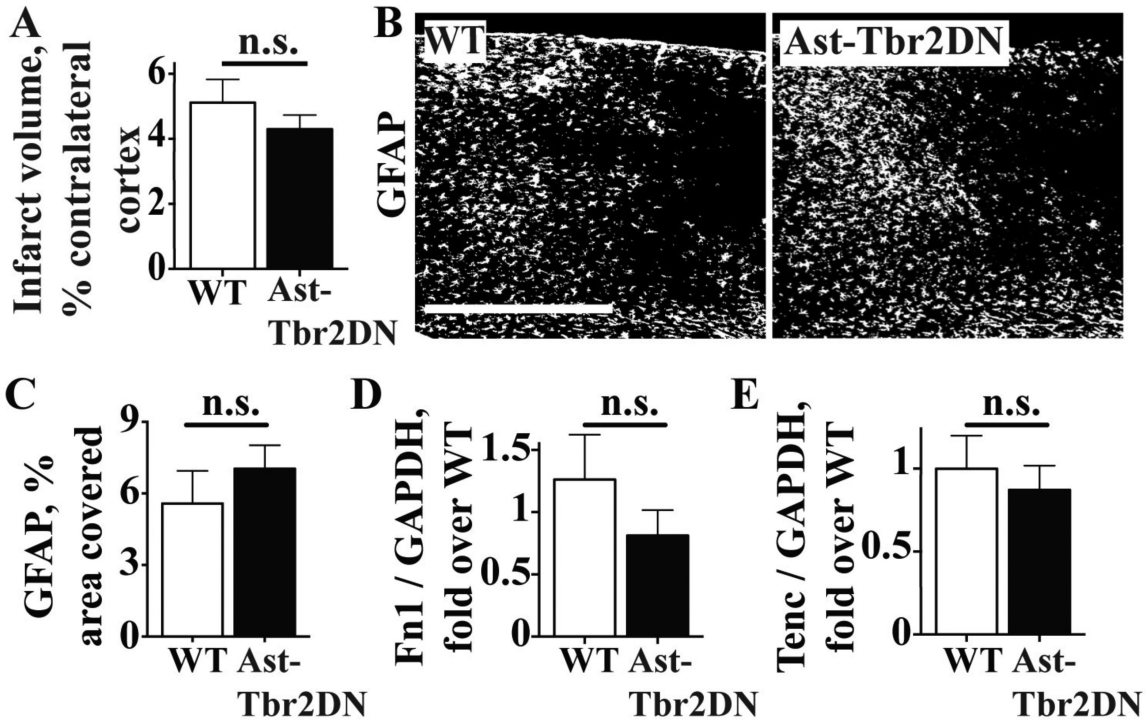

Figure 3. Inhibiting astrocytic TGFβ signaling does not affect stroke size or early astrocytic scar formation after dMCAO

A. Quantification of infarct size in Ast-Tbr2DN mice and wildtype controls. **B, C.** Representative images (**B**) and quantification (**C**) of reactive astrocyte marker GFAP expression in the peri-infarct cortex of Ast-Tbr2DN mice and wildtype controls 3 days after dMCAO. Scale bar, 500 μm. **D, E**. Quantification of glial scar components fibronectin-1 (**D**) and tenascin-C (**E**) mRNA levels 2 days after dMCAO.

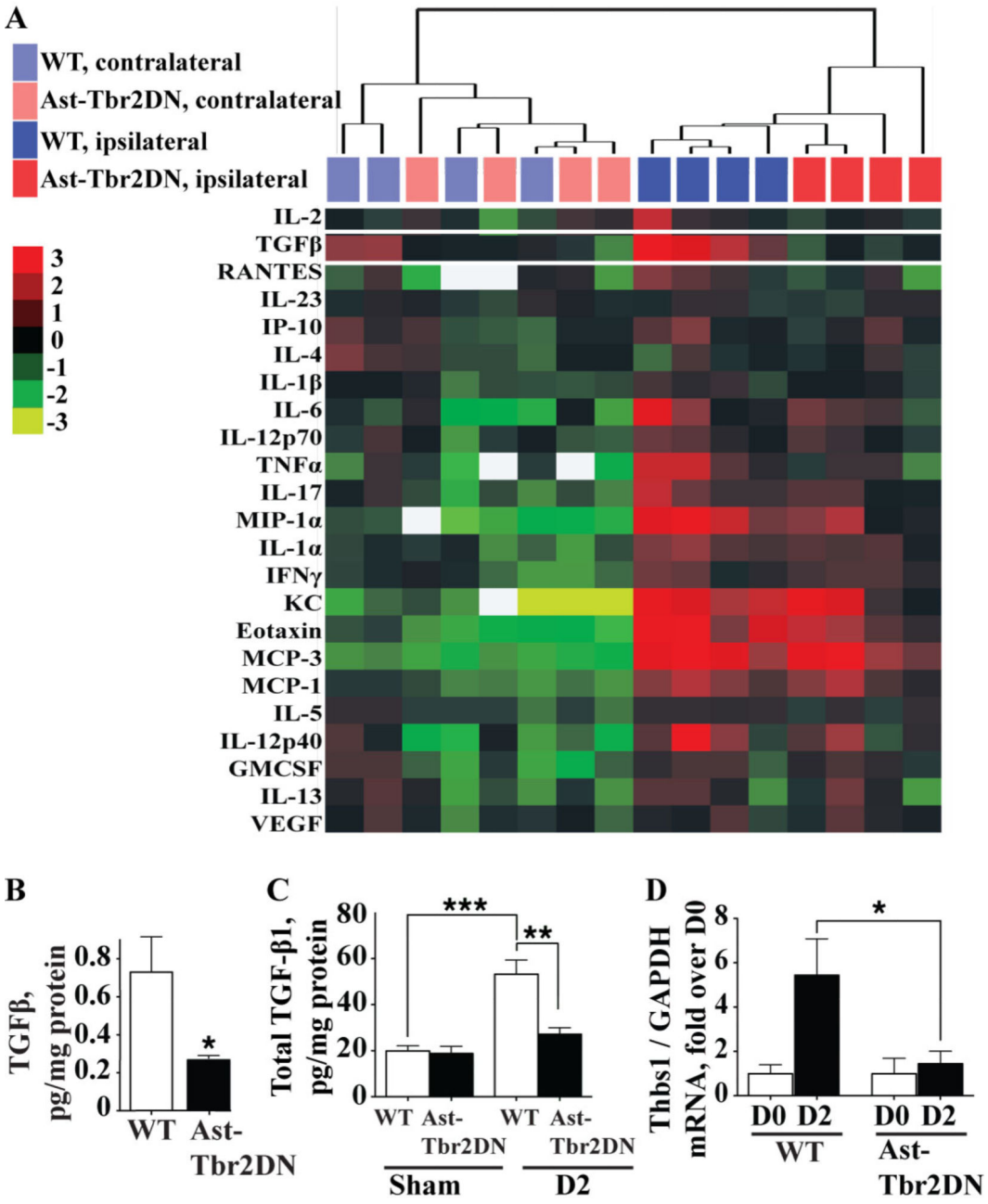

Figure 4. Astrocytic TGFβ signaling is required to upregulate functional TGFβ in the peri-infarct cortex during the subacute period after dMCAO

A. Cluster analysis of cytokine and chemokine expression in the peri-infarct and contralateral cortex of Ast-Tbr2DN mice and wildtype controls 2 days after dMCAO using a luminex assay. Heat map represents $\log_2$ levels of normalized protein expression. White squares, protein not detectable. White rectangle indicates TGF-β1, which was the only cytokine that was significantly different between Ast-Tbr2DN mice and wildtype controls. **B.** Quantification of TGFβ levels in the peri-infarct cortex of Ast-Tbr2DN mice and wildtype controls 2 days after dMCAO using a luminex assay. **C.** Quantification of TGF-β1 levels in the peri-infarct cortex at baseline and 2 days after dMCAO using ELISA. **D.**

Quantification of mRNA levels of the TGFβ activator thrombospondin-1 (Thbs1) in Ast-Tbr2DN mice and wildtype controls at baseline and 2 days after dMCAO. N=5–6 mice per group. Bars, mean ± SEM. **P*<0.05, ***P*<0.01, ****P*<0.001, Student's t test and 2-way ANOVA (interaction between genotype and time).

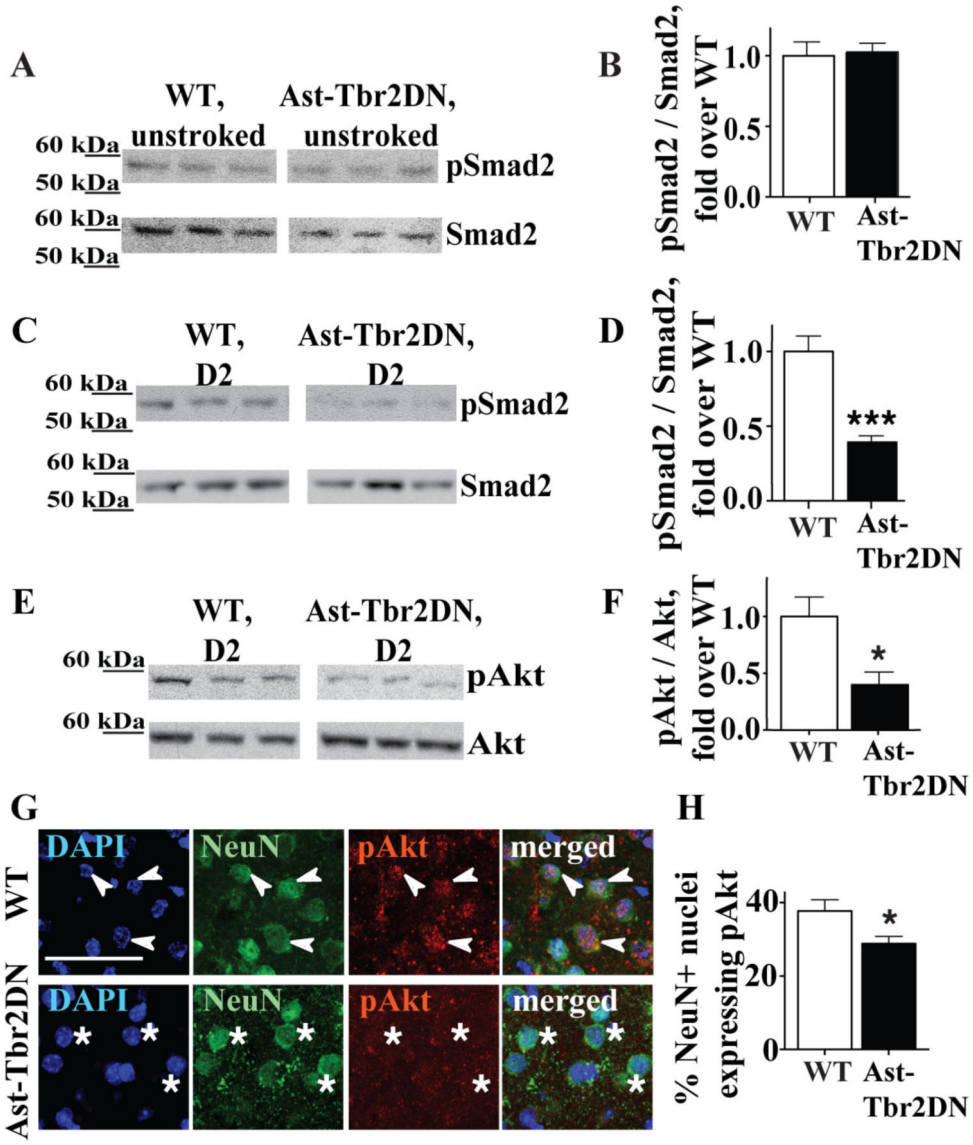

Figure 5. Inhibiting astrocytic TGFβ signaling reduces global TGFβ signaling in the peri-infarct cortex

A-D. Quantification of the TGFβ downstream signaling mediator Smad2 and its activated phosphorylated form, pSmad2, in the peri-infarct cortex of wildtype controls and Ast-Tbr2DN mice at baseline (**A, B**) and 2 days after dMCAO (**C, D**). Representative Western blot images (**A, C**) and quantification (**B, D**). **E, F.** Representative Western blot images (**E**) and quantification (**F**) of the TGFβ downstream signaling mediator Akt phosphorylation in the peri-infarct cortex of wildtype controls and Ast-Tbr2DN mice 2 days after dMCAO**. G.** Representative images of pAkt co-localization with the neuronal nuclear marker NeuN and nuclear marker DAPI in wildtype controls and Ast-Tbr2DN mice 2 days after dMCAO. Scale bar, 20 μm. Arrows, wildtype neuronal nuclei showing pAkt immunostaining. Asterisks, Ast-Tbr2DN neuronal nuclei showing no pAkt immunostaining. **H.** Quantification of pAkt co-localization with neuronal nuclear marker NeuN in wildtype

controls and Ast-Tbr2DN mice 2 days after dMCAO. N=5–6 mice per group. Bars, mean ± SEM. *P<0.05, ***P<0.001, Student's t-test.

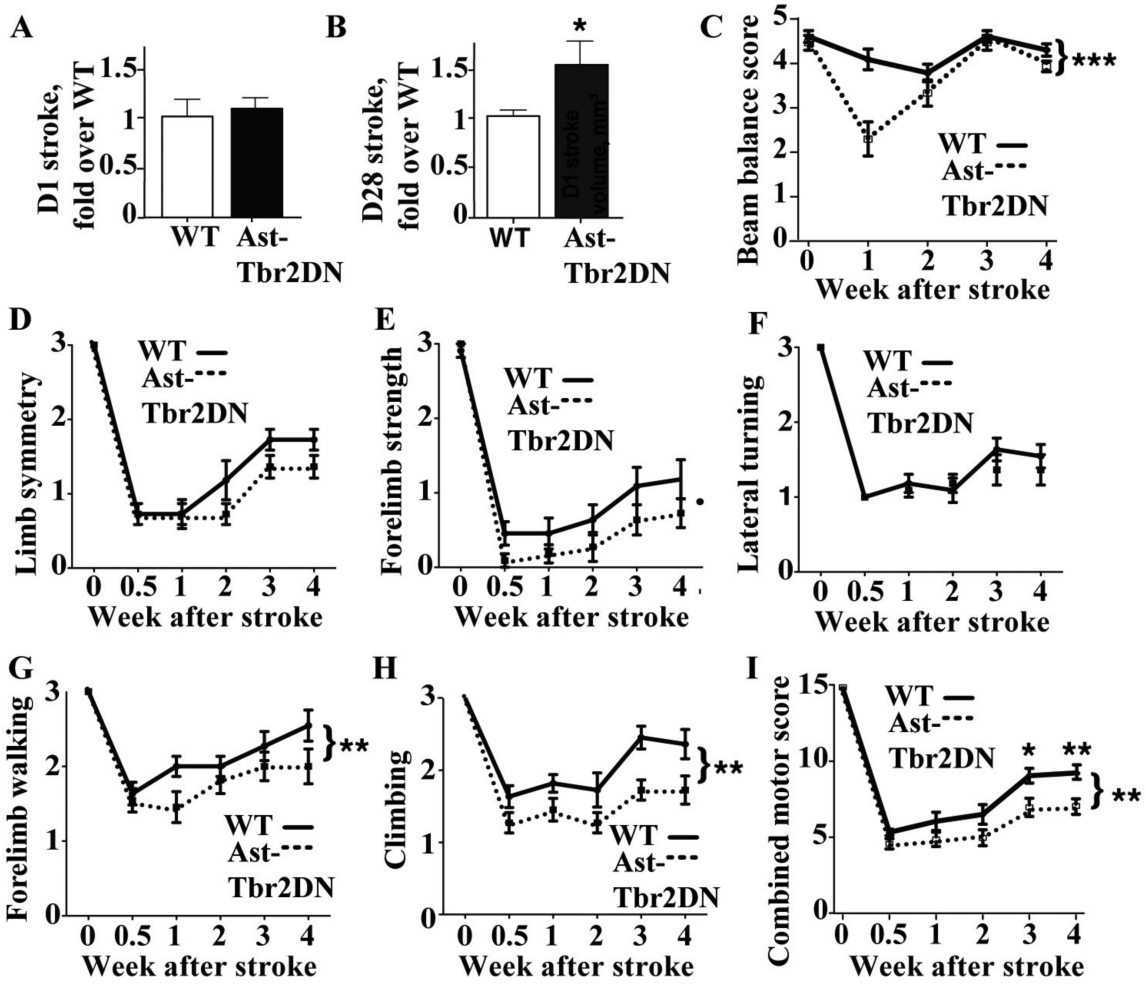

Figure 6. Ast-Tbr2DN mice develop larger infarcts and worse motor outcomes up to 4 weeks after photothrombotic stroke

A, B. Quantification of fold increase in infarct size in Ast-Tbr2DN mice compared to wildtype controls 1 day (**A**) and 28 days (**B**) after photothrombotic stroke. Bars, mean ± SEM. **P*<0.05, Student's t-test. **C.** Quantification of motor outcomes during the first four weeks after photothrombotic stroke using the Beam Balance Test. **D-H.** Quantification of motor outcomes during the first four weeks after photothrombotic stroke using tests for Limb Symmetry (**D**), Forelimb Strength (**E**), Lateral Turning (**F**), Forelimb Walking (**G**) and Climbing (**H**). **I.** Combined motor test score. N=10-12 mice per group. Bars, mean ± SEM. **P*<0.05, ***P*<0.01, ****P*<0.001, Mann-Whitney test and repeated measures ANOVA testing for differences between genotypes.

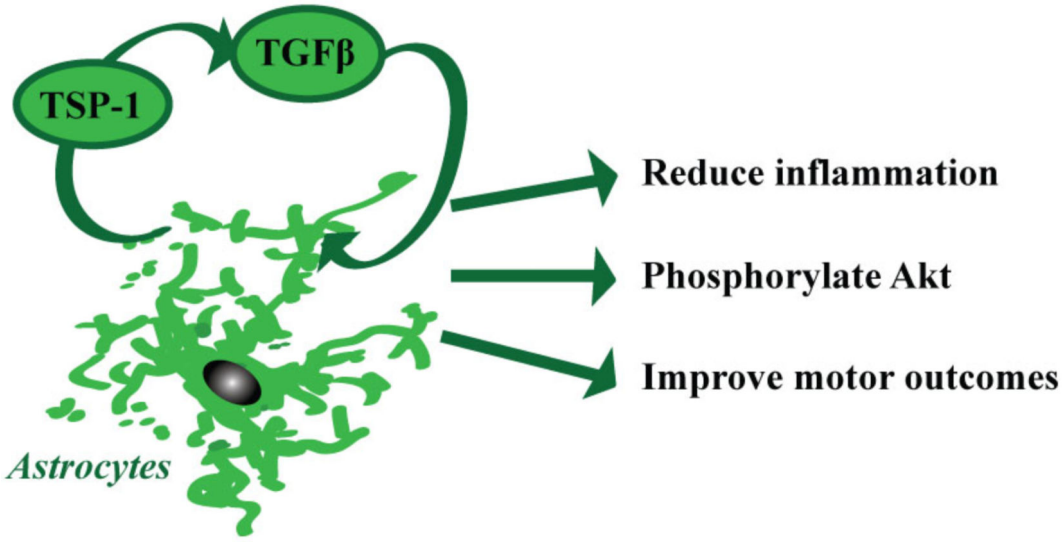

Figure 7. Model of the functions of astrocytic TGFβ signaling after stroke
TSP-1, thrombospondin-1; TGFβ, transforming growth factor beta.